35th Annual International Conference of the IEEE EMBS
Osaka, Japan, 3 - 7 July, 2013

Pixel profiling for extraction of arteriovenous malformation in 3-D CTA images

Danilo Babin, Michail Spyrantis, Aleksandra Pižurica and Wilfried Philips

Abstract— **Cerebral arteriovenous malformation (AVM) presents a great health threat due to its high probability of rupture which can cause severe brain damage or even death. For planing the embolization procedure of an AVM, the knowledge of the accurate location and size of the malformation is of utmost importance. We propose in this paper a novel AVM detection method and a blood vessel tree analysis approach using ordered thinning-based skeletonization. The main contributions are: (1) a new method of profile volume calculation to replace the distance labels in ordered skeletonization; (2) an automatic method for AVM detection and extraction, with accurate positioning and malformation size estimation. The main idea in our work is use the structural (anatomical) vessel differences and the inhomogeneities in distribution of pixel gray values to locate and extract the AVM. The algorithm takes a segmentation result as an input to perform AVM delineation. The algorithm determines the AVM region automatically, without any user interaction and independently of the segmentation algorithm used. The proposed approach is validated on brain blood vessel CTA images before and after embolization. The results obtained using the Dice coefficient comparisons, the volume percent error and the AVM center position show high accuracy of our method and indicate potentials for use in surgical planning.**

I. Introduction

Inferring the structure and position of blood vessels from medical images is crucial for surgical and diagnostic purposes. In the abundant literature on the topic a special attention is given to locating cerebral aneurysms and arteriovenous malformations (AVM). It is of utmost importance for the embolization (procedure of inserting glue into blood vessels in order to occlude them to avoid their rupture) to precisely determine the exact location of vessels going in and out of the malformation, as well as their radii, bending angles and entering (exiting) directions. The procedure is also highly influenced by the position and the size of the AVM. In this paper we address the problem of automatically locating and extracting the AVM to accurately infer its size and position. Additionally, we propose a new method for enhancing the ordered skeletonization for a more efficient shortest path calculation between points of interest in the cerebral blood vessel tree.

D. Babin, A. Pižurica and W. Philips are with Department of Telecommunications and Information Processing-TELIN-IPI-iMinds, Faculty of Sciences, Ghent University, Sint-Pietersnieuwstraat 41, B-9000 Ghent, Belgium.

M. Spyrantis is with University of Leuven - KU Leuven, Belgium.

Danilo Babin: dbabin@telin.ugent.be
Michail Spyrantis: spyrantismike@yahoo.gr
Aleksandra Pižurica: sanja@telin.ugent.be
Wilfried Philips: philips@telin.ugent.be

Recent approaches for the segmentation of cerebral blood vessels include direction-dependent level sets and vesselness measures [1]. The approach of [2] traces blood vessels based on their vesselness measures. *Vascular modeling toolkit* (VMTK) [3] is used for efficient delineation of cerebral aneurysms. A number of techniques combine various imaging approaches (and modalities) for visualization of cerebral aneurysms and AVMs, such as 3-D digital rotation angiography (3DRA) and 2-D digital subtraction angiography (DSA) [4] or 3-D and 4-D MRA images [5]. Albeit several accurate methods have been proposed to automatically analyze AVMs, none of these methods address the internal AVM structure delineation.

Center-line extraction methods are commonly divided into two groups: the tracking and the skeletonization approach. *Vessel tracking* methods track the volume or surface of a blood vessel and extract center-lines as a byproduct. The most common techniques are based on the wave front propagation for the ordered region growing [6], the connected components evolution, vessel models and the shortest path algorithm. *Skeletonization algorithms* produce center-lines from binary or gray-scale images by extracting the medial axis or ridges. *Binary skeletonization* methods operate on binary images (i.e. the segmented vessels). Many of these methods apply repeatedly the morphological thinning procedure on an object until one-pixel wide center-lines remain, using different definitions of pixel connectivity and junctions. Medial axis transform extracts center-lines by finding pixels equidistant to at least two object boundaries. *Gray-scale skeletonization algorithms* extract center-lines directly from gray-scale images. These methods usually extract and connect ridges obtained using various segmentation approaches. The most common approaches are based on an anisotropic vector diffusion [7] or morphological operations in combination with thresholding, distance maps or the watershed algorithm.

We propose a novel AVM detection approach using a multi-scale vessel density calculation. Another novelty is the introduction of a new labeling method for the ordered skeletonization based on the volume of the calculated profiles. We use our method to automatically detect and extract an AVM, with accurate estimation of its position and size. The main idea in our work is to use the structural (anatomical) vessel differences and the inhomogeneities in distribution of pixel gray values to locate and extract the AVM. The algorithm takes a segmentation as an input to perform AVM delineation. The algorithm determines the AVM region automatically, without any user interaction independently of

978-1-4577-0216-7/13/$26.00 ©2013 IEEE

the segmentation algorithm used.

II. The proposed method

We base the proposed method on our previous work on skeletonization [8] and generalized pixel profiling [9].

The proposed method is based on the following observations of blood vessels in CTA images. The AVM is an entangled blood vessel structure from which the vein drains the blood. Due to its high density of small intertwined vessels, and the fact that venous and arterial vessels merge at this position, the AVM represents a region with a higher density of vessels compared to the other parts of the cerebral blood vessel tree. The main idea in our work is use this characteristic to automatically locate and accurately extract the AVM region.

A. Ordered skeletonization

Ordered skeletonization is an iterative thinning process of a binary image, where the pixels are removed in a predefined order. The method is composed of two important principles: the pixel ordering and the pixel redundancy check algorithm. In this work we will propose an alternative to the Euclidean distance values as pixel labels for iterative thinning.

The pixel redundancy check principle is a decision rule determining if a pixel from the segmented image should be removed in the thinning process. The goal is to iteratively remove pixels to obtain one pixel wide center-lines. The redundancy check determines if a pixel can be removed from the segmented image with preserving the pixel connectivity. In this paper we use a condition from [8], where the 26-neighborhood of a pixel in a 3-D image is considered (other 3-D neighborhoods can also be used depending on the desired pixel connectivity analysis). The pixel redundancy check is performed for any pixel with more than one neighbor in the 26-neighborhood (if only one neighboring pixel exists, the processed pixel represents the end of a vessel and should not be removed). Considering the 26-neighborhood of the processed pixel, our goal is to preserve the connectivity of all neighboring pixels if the processed pixel is removed. Hence, the processed pixel $\mathbf{p}$ is considered *redundant* if all its non-zero 26-neighbors belong to a single connected component in the neighborhood. By preserving the connectivity in the neighborhood of the processed pixel, we ensure that the connectivity will be preserved in the whole binary region and the segmented image.

B. Profile volume

The order in which pixels are removed plays a crucial role in the thinning process. Various skeletonization results can be obtained using a different order of pixel removal. The order in which the pixels are removed is usually determined by the Euclidean distance transform, i.e. the minimum distance of a pixel $\mathbf{p}$ from the edge of a vessel in the segmented image:

$$r_E(\mathbf{p}) = \min_{\mathbf{q}\in\mathbb{Z}^3}(d(\mathbf{p},\mathbf{q})), \quad g(\mathbf{q}) = 0, \tag{1}$$

where $d(\mathbf{p},\mathbf{q})$ represents the Euclidean distance between the given pixels. Most usually squared values of the Euclidean distance are used as labels in ordered thinning, as depicted in Fig. 1.

The advantage of this metric is that the thinning will propagate from the vessel borders to the central parts of the vessels (where the highest values are situated). This yields a skeletonization result which represents well the medial axis of the skeletonized object.

One problem with the distance transform of a binary object is that it often results in a small range of values (Fig. 1). This means that a lot of pixels will be processed in the same thinning iteration. Pixels with the same label value (i.e. pixels which are processed in the same iteration) are removed in a "raster-scan" order. However, this thinning order is not optimal for the skeletonization of all vessel structures and causes a lot of irregularities in the shape of a skeleton with many irrelevant pixels, as shown in Fig. 2. Another problem caused by the distance calculation is that many pixels need to be processed in a single iteration. This causes an increase in computation times in case multiple iterations are done for a single label. For the purpose of a more accurate skeletonization, our goal is to define a measure that gives a more accurate pixel positioning.

We propose here a novel method for assigning pixel labels for the skeletonization thinning order. The main idea is to use the number of non-zero pixels in a wider neighborhood of the processed pixel (i.e. a volume of the neighborhood), where the size of the neighborhood is determined as in case of the Euclidean distance. We call this measure the *profile volume*. Let us define a set of non-zero pixels in the sphere-shaped neighborhood Q of a pixel $\mathbf{p}$ with size r_E :

$$Q(\mathbf{p}) = \{\mathbf{q}|\ d(\mathbf{p},\mathbf{q}) \leq r_E(\mathbf{p}),\ \mathbf{q}\in\mathbb{Z}^3,\ g(\mathbf{q}) \neq 0\}. \tag{2}$$

The profile volume is the cardinality of the non-zero pixel set:

$$v(\mathbf{p}) = |Q(\mathbf{p})|. \tag{3}$$

In this fashion we take into account the distance of the pixel from the edge and the volume of pixel's neighborhood. With the profile volume we assign pixel labels from a wider range of values (when compared to the squared Euclidean distance) and obtain a higher accuracy for the thinning process. Calculated profile volumes for a binary object are depicted in Fig. 1. Comparison of skeletonization results using squared Euclidean distance and profile volume as the thinning order labels is illustrated in Fig. 2. Our proposed method results in a more accurate skeleton image with fewer irrelevant details.

C. Profile density size and AVM extraction

As mentioned earlier, an important characteristic of an AVM is its higher density of vessel structures compared to the rest of the blood vessel tree. However, in order to extract the AVM we need to specify the size of the region (volume) in which the density of vessels will be calculated. This presents a problem since the size and volume of the AVM can vary significantly from case to case. For this reason we propose to use variable size of the region in which

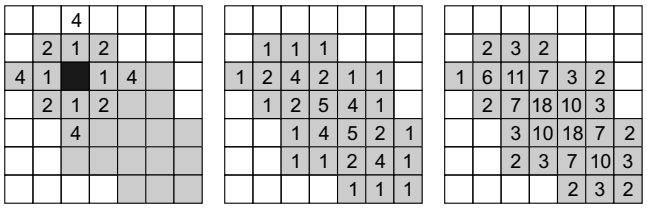

Fig. 1: Pixel labels for ordered skeletonization of a binary structure (gray pixels). Left: the squared Euclidean distance (1) for a single pixel. Middle: distance transform using the squared Euclidean distance. Range of values is small (4 distinct values), and many pixels are processed in the same thinning iteration, which results in less accurate skeletonization images. Right: labels obtained using our proposed profile volume measure. The range of values (8 distinct values) is higher than in case of the distance transform, yielding a higher accuracy in the ordered skeletonization.

Fig. 2: An ordered skeletonization of cerebral blood vessels. (a) Close-up view of segmented vessels. (b) The ordered skeletonization using the squared Euclidean distance has a lot of irrelevant details. (c) The ordered skeletonization using our proposed profile volumes yields a much more accurate skeleton with fewer irrelevant details.

the density is calculated. Moreover, since the density (of a region) has to be large enough to count as an AVM region, we allow the user to manually set the threshold value for the AVM density. For the given threshold density, we compute for each pixel in the segmented image the maximum size of the region in which the density of the vessels is higher the given threshold. We use a multi-scale neighborhood in shape of spherical layers to represent the region in which the density is computed:

$$R_i(\mathbf{p}) = \{\mathbf{q} \mid i^2 \leq d(\mathbf{p},\mathbf{q}) < (i{+}1)^2,\ \mathbf{q} \in \mathbb{Z}^3,\ i \in \mathbb{N}\}. \quad (4)$$

Let $N_i(\mathbf{p})$ denote a set of all pixels with non-zero gray value that belong to the set $R_i(\mathbf{p})$:

$$N_i(\mathbf{p}) = \{\mathbf{q} \mid \mathbf{q} \in R_i(\mathbf{p}),\ g(\mathbf{q}) \neq 0\}. \quad (5)$$

We define the profile size r_x as the maximum consecutive radius value for which the ratio of the number of non-zero value pixels $|N_i(\mathbf{p})|$ and the total number of pixels in the neighborhood $|R_i(\mathbf{p})|$ does not fall under a given density coefficient value $x \in [0,1]$:

$$r_x(\mathbf{p}) = \max\{i \mid \forall j \leq i:\ |N_j(\mathbf{p})| \geq x|R_j(\mathbf{p})|\}. \quad (6)$$

For each pixel in the segmented image, the profile density size is calculated for the chosen density coefficient x to obtain the transformed image. If the density coefficient was well chosen, the highest values in the transformed image will belong to the region of the AVM nidus. Moreover, these values will "converge" to the same location, which means that they represent the largest connected component at the given threshold value. Therefore, we propose to extract the AVM by thresholding the transformed image and extracting the largest connected component. This is illustrated in Fig. 3, where the vessels are shown with the extracted AVM region for different threshold values. For each connected component the geometric median position of all its pixels is calculated. The threshold is lowered (to get a larger AVM region) while the calculated geometric median position does not differ significantly from its previous values (in our experiments allow 2 pixels of position deviation).

III. Results

We validate our proposed algorithm for locating and extracting the AVM on three cases of cerebral vessels containing AVMs, where the onyx cast images were acquired after the embolization procedure. The onyx cast images are thresholded and used as the ground truth (the threshold is easily determined because the onyx is the brightest object in the image). We apply a hole filling algorithm on the extracted AVM region and the corresponding onyx region to suppress the influence of segmentation algorithm on obtained models (in this fashion segmentation of the inner AVM structure does not influence the comparison). In our experiments we use the density coefficient $x = 0.25$ and 2 pixels deviation of geometric median position (both of these were determined on a trial and error basis). For evaluating the obtained results we use the Dice coefficient [10], which is a set similarity measure defined as twice the ratio of intersection of two sets (set of segmented pixels and set of ground truth pixels) and the number of elements contained in both of them:

$$s(X,Y) = \frac{2|X \cap Y|}{|X| + |Y|}, \quad (7)$$

where X and Y represent the sets of segmented and ground truth pixels. Besides the Dice coefficient, we calculate the volume percent error and the distance between calculated AVM center positions. The comparison of the obtained results is given in Table I. In each case, our method was able to accurately determine the position of the AVM with slightly over-estimating the AVM volume. Fig. 4 shows two segmented blood vessel trees with extracted AVM region and a shortest path to it through arterial vessels. Our algorithm is computationally efficient with about 20 seconds execution time for a 230×256×256 data set on a 2.2 GHz processor.

IV. Conclusion

We introduced a method of profile volume calculation to replace the distance calculation in order to obtain a higher accuracy of ordered skeletonization in terms of structure representation. Moreover, we introduced and advanced multi-scale method of profile density size calculation, which we use

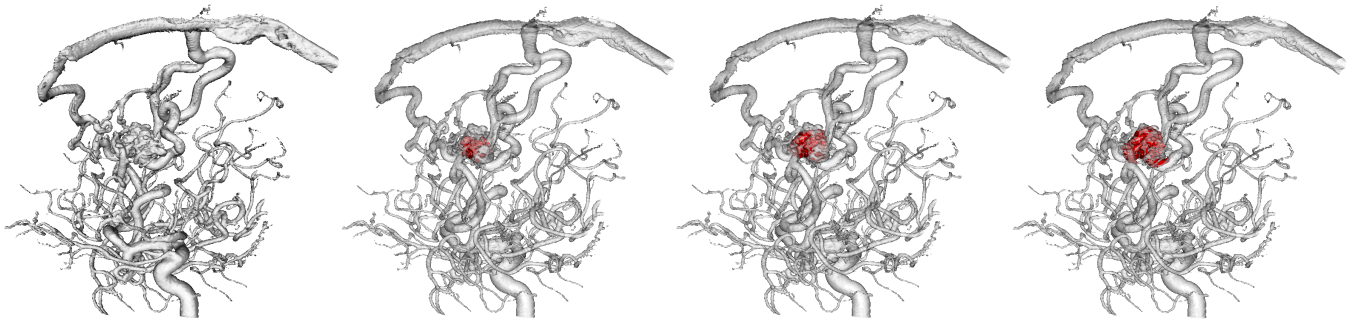

(a) (b) (c) (d)

Fig. 3: AVM extraction principle. (a) Segmented blood vessels. (b), (c), (d) Blood vessels with delineated AVM region for density coefficient $x = 0.25$ and decreasing threshold values 15000, 7500 and 2500, respectively. Note the increasing size of the delineated AVM region (red).

TABLE I: Comparisons of the filled segmented onyx cast with the filled extracted AVM segmentation

Validation	Set 1	Set 2	Set 3
Dice	0.83	0.77	0.81
Vol. % error	10	18	13
Distance (pixels)	2.99	0.98	1.73

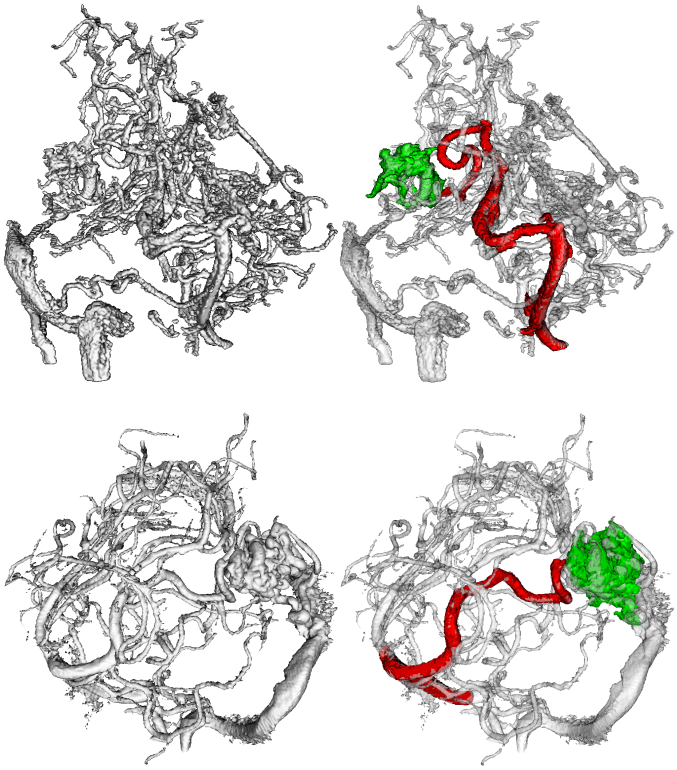

Fig. 4: Segmented cerebral blood vessels with extracted AVM (green) and a shortest path to the AVM through arterial vessels (red).

to locate and extract the AVM region. The AVM detection and delineation method was validated on real 3-D CTA data sets of cerebral vessels with the scan of onyx cast after embolization procedure. In each case the AVM position was accurately determined, with the well extracted region of the AVM. Advantage of our algorithm is that it works independently of the used segmentation algorithm. The designed application is fast and requires no manual intervention to perform delineation.

REFERENCES

[1] N. D. Forkert, S. D., I. T., J. Fiehler, E. J., H. H., and S.-R. A., "Direction-dependent level set segmentation of cerebrovascular structures," in *Progress in biomedical optics and imaging*, vol. 12, no. 31, 2011.

[2] M. Jackowski, X. Papademetris, L. Dobrucki, A. Sinusas, and L. Staib, "Characterizing vascular connectivity from microct images," in *Medical Image Computing and Computer-Assisted Intervention MICCAI 2005*, ser. Lecture Notes in Computer Science, J. Duncan and G. Gerig, Eds., vol. 3750. Springer Berlin / Heidelberg, 2005, pp. 701–708.

[3] L. Antiga and D. Steinman, "Vascular modeling toolkit," 2006.

[4] D. Hristov, L. Liu, J. R. Adler, I. C. Gibbs, T. Moore, M. Sarmiento, S. D. Chang, R. Dodd, M. Marks, and H. M. Do, "Technique for targeting arteriovenous malformations using frameless image-guided robotic radiosurgery," *International Journal of Radiation Oncology*Biology*Physics*, vol. 79, no. 4, pp. 1232–1240, 2011.

[5] N. D. Forkert, J. Fiehler, T. Illies, D. P. Mäller, H. Handels, and D. Säring, "4d blood flow visualization fusing 3d and 4d mra image sequences," *Journal of Magnetic Resonance Imaging*, 2012.

[6] C. Kirbas and F. Quek, "Vessel extraction in medical images by 3d wave propagation and traceback," in *Bioinformatics and Bioengineering, 2003. Proceedings. Third IEEE Symposium on*, march 2003, pp. 174–181.

[7] Z. Yu and C. Bajaj, "A segmentation-free approach for skeletonization of gray-scale images via anisotropic vector diffusion," in *Computer Vision and Pattern Recognition, 2004. CVPR 2004. Proceedings of the 2004 IEEE Computer Society Conference on*, vol. 1, 2004, pp. 415–420.

[8] D. Babin, J. De Bock, A. Pizurica, and W. Philips, "The shortest path calculation between points of interest in 3-d mri images of blood vessels," in *Annual Workshop on Semiconductor Advances for Future Electronics and sensors, 11th, Proceedings*. STW Technology Foundation, 2008, pp. 295–298.

[9] D. Babin, A. Pižurica, R. Bellens, J. De Bock, Y. Shang, B. Goossens, E. Vansteenkiste, and W. Philips, "Generalized pixel profiling and comparative segmentation with application to arteriovenous malformation segmentation," *Medical Image Analysis, Elsevier*, vol. 16, no. 5, pp. 991–1002, 2012.

[10] L. R. Dice, "Measures of the amount of ecologic association between species," *Ecology*, vol. 26, no. 3, pp. 297–302, 1945.